

Edge Effects on the Electronic Structures of Chemically Modified Armchair Graphene Nanoribbons

Hao Ren,¹ Qunxiang Li,^{1,*} Haibin Su,² Q. W. Shi,¹ Jie Chen,^{3,4} and Jinlong Yang^{1,†}

¹*Hefei National Laboratory for Physical Sciences at Microscale,*

University of Science and Technology of China, Hefei, Anhui 230026, P.R. China

²*Division of Materials Science, Nanyang Technological University, 50 Nanyang Avenue, 639798, Singapore*

³*Electrical and Computer Engineering, University of Alberta, AB T6G 2V4, Canada*

⁴*National Institute of Nanotechnology, Canada*

(Dated: February 2, 2008)

In this paper, we apply the first-principle theory to explore how the electronic structures of armchair graphene nanoribbons (AGNRs) are affected by chemical modifications. The edge addends include H, F, N, NH₂, and NO₂. Our theoretical results show that the energy gaps are highly tunable by controlling the widths of AGNRs and addends. The most interesting finding is that N-passivated AGNRs with various widths are metallic due to the unique electronic features of N-N bonds. This property change of AGNRs (from semiconducting to metallic) is important in developing graphene-based devices.

PACS numbers: 73.22.-f, 73.20.Hb, 72.80.Rj, 73.63.Bd

I. INTRODUCTION

Graphene, a single atomic layer of graphite with a honeycomb crystal structure, has attracted a great number of research activities.¹ Its structural properties, electrical conductance and quantum Hall effects have been investigated for making novel nanoelectronic devices.^{2,3,4} Due to the linear energy dispersion relation near the Dirac points, graphene is an interesting conductor in which electrons move like massless Dirac-fermions.³ It is now possible to make graphene nanoribbons (GNRs) with various experimental methods such as tailoring via a scanning tunneling microscopy tip,⁵ exfoliating from high oriented pyrolytic graphite,^{3,4,6} or graphitizing SiC wafers.⁷ The energy gaps of GNRs with several tens of nanometers can be measured because the growth of the energy gap is inversely proportional to the GNRs' width.⁸ There are two typical types of GNRs according to their edge configurations, either armchair or zigzag. Zigzag edge GNRs are metallic without considering the freedom of spin because the two edge states are degenerated at the Fermi level. Hydrogen-saturated armchair GNRs (AGNRs), on the other hand, are semiconductors.^{9,10} The electronic transport and magnetic properties of zigzag GNRs have also been studied by several research groups.^{9,11,12,13}

Because of the high ratio between edge and inner atoms, the electronic structure of narrow GNRs are sensitive to various edge addends. Individual carbon atoms on graphene edges are only bounded to two neighboring carbon atoms and a dangling carbon bond offers a remarkable opportunity for altering GNR's electronic properties. This edge modification can be implemented by attaching various atoms or functional groups to these dangling carbon atoms. To the best of our knowledge, edge modified AGNRs, except for the hydrogen-passivated GNRs, have not been systematically examined using Density Functional Theory (DFT). In this

paper, the electronic structures of AGNRs, with various addends including H, F, N, NO₂ and NH₂, are thoroughly investigated based on first-principle calculations. Our results show that AGNRs can be either semiconducting or metallic by changing edge chemical addends. This remarkable characteristic is very useful in making graphene-based molecule computing or sensing devices. The detailed analysis of the electronic structures can also be used to understand the underlying microscopic mechanisms of these edge effects.

II. MODEL AND METHOD

The electronic structure calculations are carried out by employing the Vienna *ab initio* simulation package with local density approximation.^{14,15} The electron-ion interactions are described based on the projected augmented wave (PAW) and the frozen core approximation.¹⁶ The energy cutoff is set to be 400 eV. Following the previous definition of AGNRs,⁹ we choose AGNRs with width $W=18, 19$, and 20 (corresponding to $3p, 3p+1$, and $3p+2$, respectively. Here, p is an integer) as examples to study three kinds of AGNRs. The schematic of a sample AGNR with width of $W=18$ is shown in Figure 1. Various addends, such as H, F, and N atoms, are connected to individual edge carbon atoms. In the NH₂ and NO₂ passivated cases, each edge carbon atom bonds to one NH₂ or NO₂ group alternatively (its neighboring carbon atom is saturated by an H atom). In our calculations, all atomic positions are allowed to relax. The convergence tolerance in energy and force is 2×10^{-5} eV and 0.02 eV/Å, respectively. The vacuum layers between two neighboring AGNR sheets and AGNR edges are set to be 12 Å and 15 Å wide, respectively. In a typical calculation, a one-dimensional periodic boundary condition along the edge direction is imposed. We choose the k-point sampling consisting of 15 uniform k-points together with the

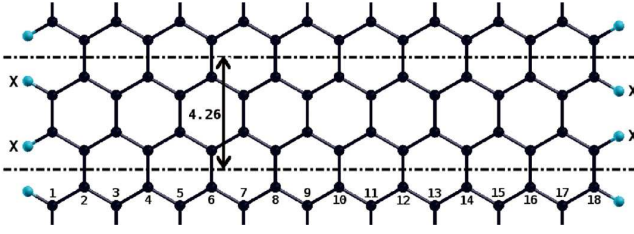


FIG. 1: (Color online) Schematic of a sample AGNR with width $W=18$. The black dots correspond to carbon atoms while the blue ones represent the addends (labeled with X, where X can be H, F, N, 2H, 2F, NO_2 , and NH_2 molecules). The distance between two dash-dotted lines is the lattice constant of one-dimensional unit-cell in the DFT calculations.

TABLE I: The calculated energy gaps (in eV) of X-AGNRs with width $w=18, 19$, and 20 . Here, “M” stands for the metallic case without E_{gap} .

W X=	H	F	2H	2F	NO_2	NH_2	N
18 E_{gap} (eV)	0.41	0.61	0.70	0.45	0.38	0.47	M
19 E_{gap} (eV)	0.61	0.35	0.10	0.15	0.57	0.38	M
20 E_{gap} (eV)	0.10	0.14	0.42	0.63	0.09	0.13	M
ΔE_f (eV) ^a	-2.29	-3.78	-1.35	-3.06	-4.05	-2.77	-1.51

^aBecause there is not much difference in bandgaps when narrow graphenes are selected, only the formation energy of AGNRs with width $w=18$ is considered. The formation energy is defined as, $\Delta E_f = \frac{1}{n}(E_{\text{tot}} - E_{\text{bare}} - \sum n_X \mu_X)$, where E_{tot} , E_{bare} , n , n_X , and μ_X is the total energy of system, the energy of unpassivated 18-AGNR, the number of chemical groups, the number of atoms of addends X and the chemical potential of X, respectively. We choose the chemical potential of H, F, N, and O as the binding cohesive energy per atom in H_2 , F_2 , N_2 , and O_2 molecules. This definition would be a appropriate measurement of the stability in passivated AGNRs. The formation energy of NO_2 and NH_2 passivated 18-AGNRs per group is defined as $\Delta E_f = \frac{1}{2}(E_{\text{tot}} - E_{\text{bare}} - \sum n_X \mu_X - 2 \times \Delta E_f(\text{H}))$, where $\Delta E_f(\text{H})$ is the formation energy of H-passivated 18-AGNR.

Γ point.

III. RESULTS AND DISCUSSIONS

We first choose the well-studied hydrogen passivated AGNRs^{9,17} as a basis to validate our numerical results. The calculated band structures of three kinds of hydrogen passivated AGNRs are plotted in Figure 2 (a). The corresponding bandgaps together with the optimized C-C distances at the edge are listed in Table I. Our results show that all three kinds of AGNRs are semiconductors with direct band gaps at the Γ point. The figure clearly shows that the AGNR with width $W = 3p + 1$ has the largest energy gap, while the AGNR with width $W=3p+2$ has the smallest one. Our calculated bandgaps are 0.41, 0.61, and 0.10 eV for the H passivated AGNRs with width $W=18, 19$ and 20 , respectively. These results agree well with the previously reported results^{9,17}.

Next, we examine the electronic structures of AGNRs with F atoms passivated at both edges. The cal-

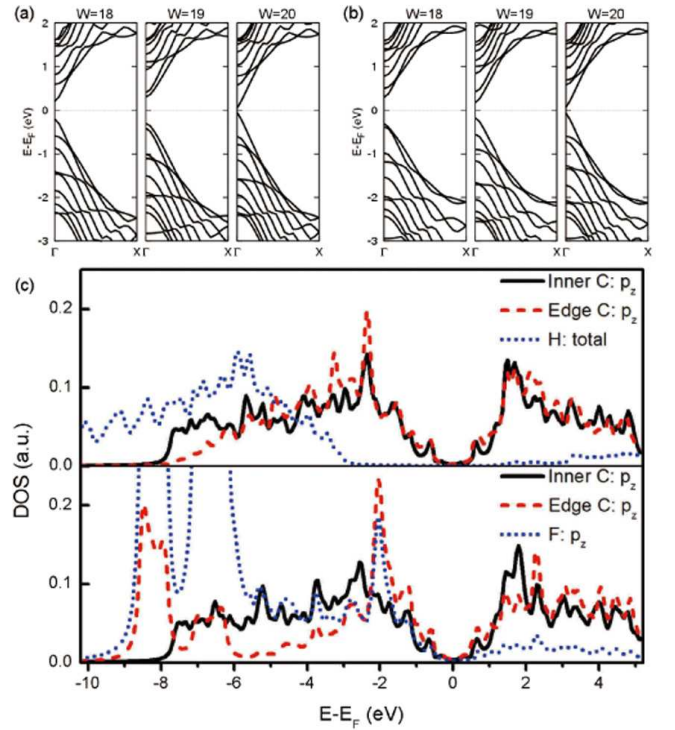


FIG. 2: (Color online) (a) and (b) show the band structures of H and F-passivated AGNRs with width $W=18, 19$, and 20 , respectively. (c) The projected density of states (PDOS) of H (upper panel) and F (lower panel) passivated AGNRs with width $W=18$.

culated band structures are plotted in Fig. 2 (b) and the bandgaps are listed in Table I. Similar to the H-passivation cases, all F-passivated AGNRs are semiconductors. However, the effects of GNR width on bandgaps is clearly different. For instance, the F-passivation makes the band gap of the AGNR with width $W=18$ ($3p$) to be the largest (0.61 eV), while the gap of the AGNR with width $W=20$ ($3p+2$) is the smallest (0.14 eV). It is important to note that the bandgaps of the AGNRs (width $W=20$) with the smallest gaps remain as the smallest even after passivation. However, AGNRs with the largest bandgaps behave differently and depend on elements used for passivation. We also would like to know what happens if individual edge carbon atoms connect to two H or F atoms instead of one H or F atom. Intuitively, the sp^2 hybridization of edge carbon atoms is converted into sp^3 hybridization. The effective AGNR width is therefore reduced by 2. In other words, the effective width becomes 17 for both double H- and F-passivated AGNRs when their initial width is $W=19$. Because the effective width of 17 fits $3p+2$, the corresponding double H- and F-passivated AGNRs have the smallest energy gap (about 0.1 eV). The largest gaps are 0.70 eV for double H-passivated AGNRs with $W=17$ or effective $W=16$ ($3p+1$). Similarly, 0.63 eV for of double F-passivated AGNRs with $W=20$ or effective $W=18$ (a $3p$ case). These results are consistent with the width de-

pendent energy gap features in single F- or H-passivated AGNRs.

It is instructive to compare the DFT results with the tight-binding approximation (TBA) data. Wang *et al.* have reported that energy gaps can be tuned by changing edge hopping parameters.¹⁷ Son *et al.* have also showed that the energy gaps of H-passivated AGNRs can be reproduced via TBA simulations. In their simulations, edge hopping parameters can be increased by decreasing the bond length of C atoms at edges.⁹ Although the geometric deformations of carbon networks are almost the same between H-passivated GNRs and F-passivated ones, the bandgaps surprisingly show distinct dependence on the width of AGNRs. According to the TBA parameters adopted in these analytical calculations of the edge modified GRNs,¹⁸ the π_{pp} hopping integrals, representing the coupling between p_z orbital of two neighboring carbon atoms, increases as the C-C distance decreases. However, this statement is invalid when the bond length substantially decreases so that the hybridization between two carbon atoms becomes perturbed. From the PDOS of the H-passivated AGNRs, we can see that the peaks of p_z orbital of edge C atoms almost coincide with that of the inner C atoms below the Fermi level [see Fig2(c)]. The π_{pp} bonding remains unchanged during the H-passivation of edge C atoms. The modification of energy gaps caused by H atoms could be explained based on the geometry deformation. Interestingly, the p_z orbital of both edge C atoms and F addends have peaks at -8.5 eV below the Fermi energy. The peak position of the edge C atoms, however, decreases significantly compared to the inner C atoms from -6.0 to -2.3 eV below the Fermi energy, which is still within the energy range of π bonding in F-passivated AGNRs. That is to say, the p_z orbital of edge C atoms in the F-passivated cases form chemical bonds with the neighboring C atoms and the F atoms. Consequently, the hopping parameters decrease. If we choose the hopping parameter to be 84% of -2.7 eV (the typical hopping integral of sp^2 carbon system), the energy gaps of AGNRs with width $W=18, 19$, and 20 are $0.65, 0.35$, and 0.13 eV, respectively, which agree excellently with results obtained by DFT. This observation demonstrates that the electronic structures of AGNRs can be controlled by edge chemical modifications.

NO_2 and NH_2 radicals are widely used as anchoring or side groups for making single molecular junctions in molecular electronics.^{19,20,21} In the next calculations, NO_2 and NH_2 are attached to AGNRs and we investigate how these addends impact GNR electronic structures. Figs. 3 (a) and (b) show their band structures. Figs. 3 (c) and (d) show their optimal geometric structures. The NH_2 group lies in the AGNR plane for NH_2 passivated GNRs, while, for NO_2 passivated GNRs, the dihedral angle is 59° between AGNR and NO_2 plane. According to the projected DOS in Figure 4, their electronic structures also exhibit different features. For the NH_2 -passivated AGNRs, the nitrogen atom forms one sp^2 orbital, which bonds to two hydrogen and one edge carbon atom. The

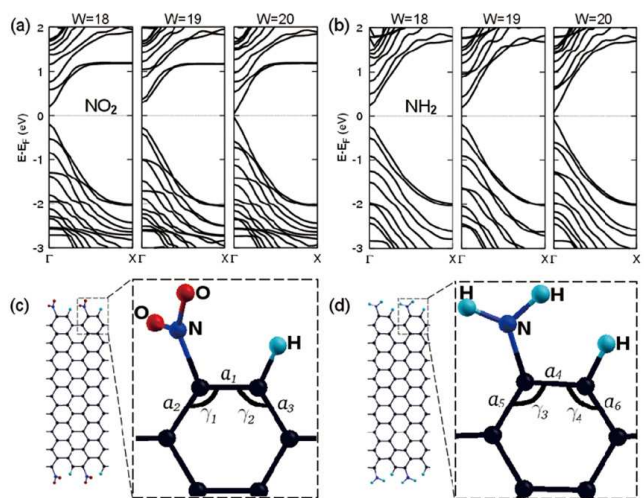


FIG. 3: (Color online) Band structures of NO_2 - and NH_2 -passivated AGNRs with width $W = 18, 19$, and 20 are shown in (a) and (b), respectively. The edge relaxed geometric structures of NO_2 and NH_2 are shown in (c) and (d). The relaxed bond lengths from a_1 to a_6 are $1.36, 1.40, 1.39, 1.37, 1.42$, and 1.37 Å, respectively, and the bond angles from γ_1 to γ_4 are $122.8^\circ, 120.6^\circ, 117.5^\circ$, and 126.6° , respectively.

remaining p_z orbital of the nitrogen atom bonds nicely to the p_z orbital of the edge carbon. For the NO_2 case, the π orbital in the NO_2 plane does not bond well to the sp^2 framework of AGNRs because the NO_2 plane twists out of the AGNR sheet. Comparing to the bandgaps of H- and F-passivated AGNRs, it is interesting to note that the bandgap of NO_2 is close to that of H, while the bandgap of NH_2 is similar to that of F. The fundamental cause is attributed to the influences of the carbon p_z orbital. Neither H nor NO_2 forms a bond with the carbon p_z orbital, but both F and NH_2 facilitate bonding directly to carbon p_z orbital. Hence, it is expected that substantial charge transfer occurs together with the non-negligible change in the hopping integral near the edges of both F- and NH_2 -passivated AGNRs.

Very recently, N-rich Oligoacenes were considered to be candidates for n-channel organic semiconductors.²² N-doped carbon nanotubes and nanofibers have also been synthesized and investigated intensively over the past years.^{23,24,25,26} These investigations motivate us to examine the N-passivated AGNRs. According to the calculated formation energy in Table 1, it is possible to attach one N atom to each C atom along the edges as an addend. Interestingly, two neighboring N addends can form an N-N dimer and form an optimal structure. The N-N bond length is 1.30 Å, which is 0.20 Å longer than that of N-N bond length in N_2 molecule. More importantly, a semiconductor-to-metal transition is observed for all N-passivated AGNRs and this transition is independent of AGNR widths. To explore the cause at the microscopic scale, the band structures of N-passivated AGNRs with various graphene widths and partial projected DOS

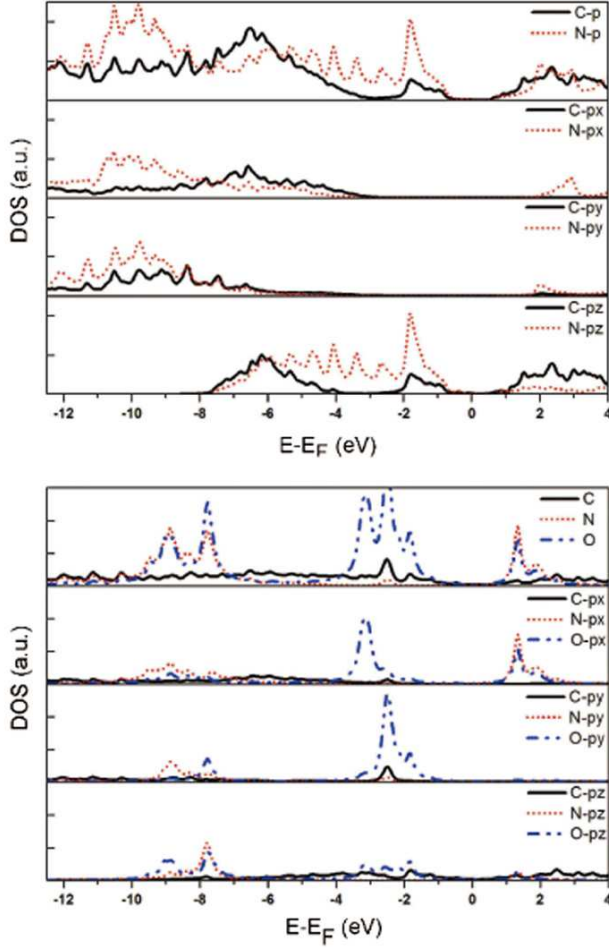


FIG. 4: (Color online) (a) Partial density of states (PDOS) of the edge C, and N in NH₂-passivated AGNRs. (b) PDOS of the C, N, and O atoms in NO₂-AGNRs. Here, W=18.

on N atoms of AGNR with width W=18 are presented in Figs. 5(a) and 5(b), respectively. Clearly, the DOS near the Fermi level is impacted by N addends. The edge N atom has 5 valence electrons. Two of them stay as a lone-pair, which locates in the AGNR's plane with the direction pointing outwards. The occupied band labeled with "A" in Fig. 5(a) has the same features as those of lone-pair electrons. The other three electrons exhibit sp²-like hybridization. Two of the sp² hybridized orbital pair with the neighboring C and N atoms to form two σ bonds, while the last electron acts as a π electron. We would like to emphasize that the metallic state of N-passivated AGNRs is predominantly contributed by the edge states of N addends. There are two reasons attributed to AGNR's semiconducting to metallic transition. i) the N-N bond is mainly composed of 2s and 2p_y orbitals. The energy of the band with N 2p_z is above the Fermi surface, which means that N 2p_z electrons fill the carbon π^* bands and push the Fermi surface inside the carbon's π^* bands. ii) the lone-pair electrons of N atoms are mainly in N 2p_x bands and the top part of 2p_x

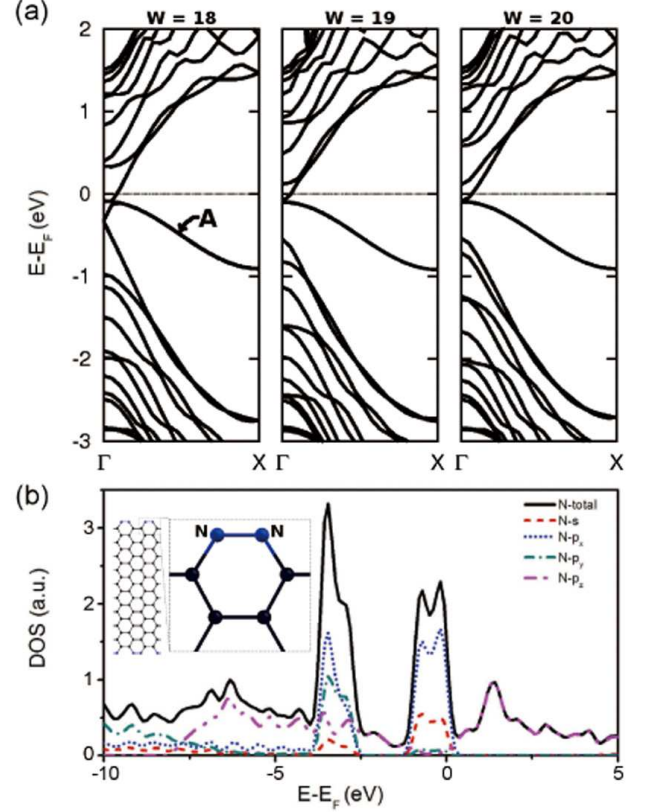


FIG. 5: (Color online) (a) Band structures and DOS of N-passivated AGNRs with width W = 18, 19, and 20, respectively. Here, the total DOS and projected DOS on N atoms are labeled with solid and dashed lines. (b) Partial projected DOS on N atoms of N-passivated AGNRs with width W=18. The relaxed geometry is shown in the inset in Fig.(b)

bands pass the Fermi surface. This feature contributes to the semiconducting to the metallic transition. Clearly, edge N-N addends extend the sp² network of AGNRs and thus the effective width (or the number of sp² dimer lines) of N-passivated AGNRs increases by 2 (coming from two edge sides). Apart from "A" band, the band structures of N-passivated AGNRs with width W are similar to those of H or F-passivated AGNRs with width W + 2 except that the Fermi level shifts upwards and cross the lowest unoccupied bands, which leads to the semiconductor-to-metal transition.

IV. CONCLUSION

In summary, we perform the first-principle calculations on the electronic structures of AGNRs with various edge chemical modifications. We find that the energy gap can be tuned to be either metallic or semiconducting by attaching different chemical functional addends. After AGNRs are passivated by H, F, NH₂, and NO₂, the GNRs with the smallest bandgaps (i.e. W=20) remain to have the smallest bandgaps. However, AGNRs that have the

largest bandgaps behave differently and the gaps depend on the type of elements used for passivation. H and F have similar bandgaps to NO₂ and NH₂, respectively, which can be explained based on the bonding of the carbon p_z orbital. The fascinating observation is that AGNRs passivated by attaching N atoms can change from semiconducting to metallic material regardless of AGNR width. This result is analyzed in detail based on its electronic structure. The unique electronic structure of the N-N bond, which is responsible for semiconductor-to-metal transition, is explained based on its $2s$ and $2p_y$ orbital, and the lone-pair of $2p_x$. This tunable character of AGNRs is useful in developing graphene-based molecule electronic devices in the near future.

ACKNOWLEDGMENTS

This work was partially supported by the National Natural Science Foundation of China under Grant Nos.

20773112, 10574119, 50121202, and 20533030, by National Key Basic Research Program under Grant No. 2006CB922004, by the USTC-HP HPC project, and by the SCCAS and Shanghai Supercomputer Center. Work at NTU is supported in part by a COE-SUG grant (No. M58070001) and A*STAR SERC grant (No. 0521170032). Jie Chen would like to acknowledge the funding support from the Discovery program of Natural Sciences and Engineering Research Council of Canada under Grant No. 245680.

-
- * Corresponding author. E-mail: liquan@ustc.edu.cn
 † Corresponding author. E-mail: jlyang@ustc.edu.cn
- ¹ A. K. Geim and K. S. Novoselov, *Nature Mater.*, **6**, 183 (2007).
 - ² K. S. Novoselov, A. K. Geim, S. V. Morozov, D. Jiang, Y. Zhang, S. V. Dubonos, I. V. Grigorieva, and A. A. Firsov, *Science* **306** 666(2004).
 - ³ K. S. Novoselov, A. K. Geim, S. V. Morozov, D. Jiang, M. I. Katsnelson, I. V. Grigorieva, S. V. Dubonos, and A. A. Firsov, *Nature* **438**, 197 (2005).
 - ⁴ Y. B. Zhang, Y. W. Tan, H. L. Stormer, and P. Kim, *Nature* **438**, 201 (2005).
 - ⁵ H. Hiura, *Appl. Surf. Sci.* **222**, 374 (2004).
 - ⁶ J. S. Bunch, A. M. van der Zande, S. S. Verbridge, I. W. Frank, D. M. Tanenbaum, J. M. Parpia, H. G. Craighead, and P. L. McEuen, *Science* **315**, 490 (2007).
 - ⁷ C. Berger, Z. M. Song, X. B. Li, X. S. Wu, N. Brown, C. Naud, D. Mayou, T. B. Li, J. Hass, A. N. Marchenkov, E. H. Conrad, P. N. First, and W. A. de Heer, *Science* **312**, 1191 (2006).
 - ⁸ M. Y. Han, B. Öylmaz, Y. B. Zhang, and P. Kim, *Phys. Rev. Lett.* **98**, 206805 (2007).
 - ⁹ Y.-W. Son, M. L. Cohen, S. G. Louie, *Phys. Rev. Lett.* **97**, 216803(2006); Y.-W. Son, M. L. Cohen, S. G. Louie, *Nature* **444**, 347(2006).
 - ¹⁰ H. X. Zheng, Z. F. Wang, T. Luo, Q. W. Shi, and J. Chen, *Phys. Rev. B* **75**, 165414 (2007).
 - ¹¹ O. Hod, V. Barone, J. E. Peralta, and G. E. Scuseria, *Nano Lett.* **7**, 2295(2007).
 - ¹² D. Gunlycke, J. Li, J. W. Mintmire, and C. T. White, *Appl. Phys. Lett.* **91**, 112108(2007).
 - ¹³ D. Jiang, B. G. Sumpter, and S. Dai, *J. Chem. Phys.* **126**, 134701 (2007).
 - ¹⁴ G. Kresse and J. Furthmüller, *Phys. Rev. B* **54**, 11169 (1996); *Comput. Mat. Sci.* **6**, 15 (1996); G. Kresse and J. Hafner, *Phys. Rev. B* **47**, R558 (1993); *Phys. Rev. B* **48**, 13115 (1993).
 - ¹⁵ J. P. Perdew and Y. Wang, *Phys. Rev. B* **45**, 13244 (1992); *Rev. B* **49**, 14251 (1994).
 - ¹⁶ P. E. Blöchl, *Phys. Rev. B* **50**, 17953 (1994); G. Kresse and J. Joubert, *Phys. Rev. B* **59**, 1758 (1999).
 - ¹⁷ Z. F. Wang, Q. X. Li, H. X. Zheng, H. Ren, H. B. Su, Q. W. Shi, and J. Chen, *Phys. Rev. B* **75**, 113406 (2007).
 - ¹⁸ D. Porezag, Th. Frauenheim, Th. Köler, G. Seifert, and R. Kaschner, *Phys. Rev. B* **51**, 12947 (1995).
 - ¹⁹ L. Venkataraman, J. E. Klare, C. Nokolts, M. S. Hybertsen, and M. L. Steigerwald, *Nature* **442**, 904 (2006).
 - ²⁰ L. Venkataraman, Y. S. Park, A. C. Whalley, C. Nuckolls, M. S. Hybertsen, and M. L. Steigerwald, *Nano Lett.* **7**, 502 (2007).
 - ²¹ A. Star, T.-R. Han, J.-C. P. Gabriel, K. Bradley, and G. Grüer, *Nano Lett.* **3**, 1421 (2003).
 - ²² M. Winkler and K. N. Houk, *J. Am. Chem. Soc.* **129**, 1805(2006).
 - ²³ M. Terrone, A. J. M. Endo, A. M. Rao, Y. A. Kim, T. Hayashi, H. Terrones, J.-C. Charlier, G. Dresselhaus, and M. S. Dresselhaus, *Mater. Today* **7**, No. 10, 30 (2004).
 - ²⁴ Z. Weng-Seih, K. Cherrey, N. G. Chopra, X. Blase, Y. Miyamoto, A. Rubio, M. L. Cohen, S. G. Louie, A. Zettl, and R. Gronsky, *Phys. Rev. B* **51**, 11229 (1995).
 - ²⁵ K. Harigaya, *Jpn. J. Appl. Phys.* **45**, 7237 (2006).
 - ²⁶ T. Yoshioka, H. Suzuura, and T. Ando, *J. Phys. Soc. Jpn.* **72**, 2656 (2003).